Available online at www.sciencedirect.com
ScienceDirect
C. R. Physique 9 (2008) 903–910
COMPTES RENDUS PHYSIQUE
http://france.elsevier.com/direct/COMREN/

Physics/Surfaces, interfaces, films

# Application of negative velocity dispersion curves to the distinction between layer and substrate Rayleigh waves

Zahia Hadjoub [a], Ibtissem Touati [a], Malika Doghmane [a,b], Abdellaziz Doghmane [a,*]

[a] *Laboratoire des semi-conducteurs, département de physique, faculté des sciences, Université Badji-Mokhtar, Annaba, BP 12, 23000 Algeria*
[b] *Département des sciences exactes, faculté des sciences et de l'ingénierie, Université du 08 Mai 1945, 24000 Algeria*

Received 16 November 2007; accepted after revision 11 August 2008

Available online 14 September 2008

Presented by Jacques Villain

**Abstract**

This work concerns the investigation of loading layers/substrate structures in order to determine the critical thickness at which Rayleigh wave characteristics of layers can be completely distinguished from those of the substrates. To do so, we first calculate Rayleigh velocity dispersion curves of several thin film materials (about thirty) deposited on different slow and fast substrates (Be, $Al_2O_3$, AlN, Si, $SiO_2$, Mg, SiC, TiN, WC and Pyrex). Then, from the beginning of curve saturation (corresponding to the onset of intrinsic layer characteristics) we deduced normalized thickness transition for all layers/substrates combinations. Thus, we were able to deduce an analytical linear expression relating the critical thickness to combined effects of densities and velocities of both layers and substrates. Such a simple relation can be used, as an alternative method, to predict the transition critical thickness for any layer/substrate combination without the usual lengthy calculation of dispersion curves. ***To cite this article: Z. Hadjoub et al., C. R. Physique 9 (2008).***


**Résumé**

**Application des courbes de dispersion négative des vitesses pour la distinction de l'onde de Rayleigh dans le film de celle du substrat.** Ce travail concerne l'investigation des structures couches minces/substrats vérifiant l'effet de charge dans le but de déterminer l'épaisseur critique à partir de laquelle la vitesse de l'onde de Rayleigh de la couche peut être complètement dissociée de celle du substrat. Ainsi, nous avons tout d'abord calculé les courbes de dispersion des vitesses de Rayleigh d'un grand nombre de films (une trentaine) déposés sur plusieurs substrats lents et rapides (Be, $Al_2O_3$, AlN, Si, $SiO_2$, Mg, SiC, TiN, WC et Pyrex). Ensuite, à partir du début de la saturation de chaque courbe (correspondante au seuil des caractéristiques intrinsèques du film) nous avons déterminé l'épaisseur normalisée de transition pour toutes les combinaisons films/substrats. Ainsi, il nous a été possible d'établir une relation analytique linéaire reliant cette épaisseur aux effets combinés des vitesses et densités des films et substrats. Cette relation, peut être utilisée en tant que méthode alternative directe pour prédire l'épaisseur critique de la transition pour toute structure film/substrat et éviter les calculs habituels fastidieux des courbes de dispersion. ***Pour citer cet article : Z. Hadjoub et al., C. R. Physique 9 (2008).***


*Keywords:* Thin films; Elastic properties; Velocity dispersion; Surface acoustic waves; Loading effect

* Corresponding author.
*E-mail address:* a_doghmane@yahoo.fr (A. Doghmane).

1631-0705/$ – see front matter 
doi:10.1016/j.crhy.2008.08.001

*Mots-clés :* Couches minces ; Propriétés élastiques ; Dispersion de la vitesse ; Ondes acoustique de surface ; Effet de charge

## 1. Introduction

Elastic properties of layer/substrate combinations have attracted much attention in recent years by many research groups due to not only the growing importance of layered structures in both theoretical and applied studies, but also to their present and potential roles in several technological, industrial and scientific fields. When a film is deposited on a substrate to improve the hardness and/or thermal properties of surfaces, the determination of mechanical properties of the thin layer is not a trivial task but one requiring sophisticated equipment and techniques. Therefore, one has to consider that in the frequency range commonly used, the large values of the acoustic wavelength, compared to the film thickness, require a careful consideration of the effect of the substrate on the propagation of the surface acoustic wave, SAW. Hence, the propagation properties of SAWs in layered structure are more complicated than in nonlayered structure.

The properties of layer/substrate combinations are characterized by what is known as dispersion behavior: surface waves become dispersive, i.e. the SAW velocity is a function of both frequency, $f$, and layer thickness, $h$, and elastic parameters [1–3]. Velocity dispersion curves could be negative (loading effect) or positive (stiffening effect) depending on the layer's bulk material having greater or lesser SAW velocity with respect to the substrate. It is worth noting that 'negative dispersion' is conventionally used to designate curves whose initial slope is negative and the wave velocity begins to decease as a function of frequency and/or layer thickness below the Rayleigh velocity of the substrate. In the case of loading effect, an unlimited number of Rayleigh-like modes and Love modes can exist, depending on the layer-substrate combination and the frequency-thickness, $fh$, product. For the lowest mode, called the Rayleigh mode, the dispersion curve starts at the Rayleigh velocity of the substrate, $V_{RS}$, and as the product $fh$ increases the velocity monotonically decreases to asymptotically approach the Rayleigh velocity appropriate to the layer material, $V_{RL}$. Most reported investigations on loading effects are concerned with the behavior of the whole dispersion curve [4–6] with less theoretical and experimental work reported on the initial slope of decreasing regions [7–10].

However, the critical thickness at which the Rayleigh wave propagates, completely, in the layer without any substrate effects, i.e. the transition position separating decreasing region from saturated region, has not been so clearly defined and not well studied. Moreover, the difficulty in investigating thin films is to dissociate their characteristic velocities from those of the substrates onto which they are deposited. Hence, it is the aim of this work to consider the propagation of a SAW near the transition point for loading layers; this is accomplished via the investigation of velocity dispersion curves and the determination of the acoustic parameters influencing the critical layer thickness at which elastic characteristics alter from those of the whole structure to that of the thick layer. An analytical formula to predict, in a direct way, the onset of such behavior is finally proposed.

## 2. Materials and methodology

Calculations were carried out for several substrates (AlN, $Al_2O_3$, Be, Mg, Pyrex, Si, SiC, $SiO_2$, TiN and WC) over which many loading layers (Al, AlN, $Al_2O_3$, Cr, Cu, Constantan, Fe, Heavy flint, Inconel, Mg, MgO, Mo, Ni, Monel, Pyrex, Quartz, SiC, $SiO_2$, $Si_3N_4$, Stainless steel, Ti, TiN, V, W, Zircolay, Zn, ZnO and Zr) were deposited. This great number of layers as well as substrates (more that two hundred combinations) was chosen in order to cover the largest possible spectrum of propagating SAW velocities in real materials. For every layer/substrate configuration, the loading effect is verified, i.e., the SAW velocity in the layer is less than that in the substrate.

### *2.1. Calculation procedure*

For each layer/substrate combination, the calculation procedure consists of several steps that have been described in detail elsewhere [7,11,12] and will not be reiterated here. Therefore, we only summarize them as follows:

(i) calculating acoustic materials signature, also known as $V(z)$ curves, from the angular spectrum model [13] under normal operating conditions (water couplant, 50° half-opening angle and 142 MHz operating frequency) for which Rayleigh mode dominates in a scanning acoustic microscope, SAM [11,12];

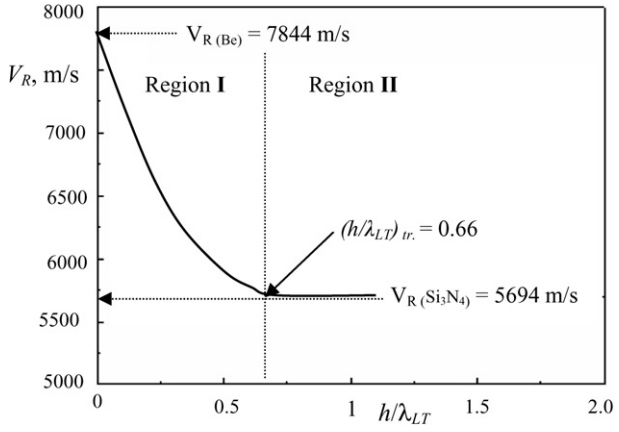


Fig. 1. Velocity dispersion curves for $Si_3N_4$/Be; the arrow indicates the normalized thickness transition, $(h/\lambda_{LT})_{tr}$, beyond which the SAW propagates completely in $Si_3N_4$.

(ii) determining Rayleigh velocities via fast Fourier transform treatment of these periodic $V(z)$ curves [11,12];
(iii) repeating the above steps for many layer thicknesses ranging from zero to twice the wavelength of the transverse waves propagating in the layer ($2\lambda_{LT}$);
(iv) plotting the dispersion curves, i.e. Rayleigh velocities, $V_R$, versus normalized thickness, $h/\lambda_{LT}$.
(v) applying the above steps to the determination of the transition thickness for every plotted dispersion curve.

### *2.2. Application*

In order to illustrate the determination procedure of the transition thickness, we apply the previous steps [(i)–(v), in Section 2.1] to a real structure, $Si_3N_4$/Be, which shows identical behavior to all other investigated layer/substrate configurations. The calculated results are displayed in Fig. 1 (solid line), in terms of Rayleigh velocity as a function of normalized thickness. It should be noted that a similar behavior was experimentally and theoretically reported for identical loading layers/substrate structures [7,8,14–17]. To facilitate later discussions, it would be more convenient to divide the curve into two distinct regions.

Region I: for small values of $h/\lambda_{LT}$ (from 0 to 0.66), as the thickness increases, Rayleigh velocity decreases sharply from its highest value $(V_R)_{Be} = 7844$ m/s representing that of Be substrate free surface. This region corresponds to the characteristics of the whole layer/substrate structure.

Region II: for large values of $h/\lambda_{LT}$, the Rayleigh velocity tends asymptotically towards a constant value. Since the threshold of the saturation region corresponds to $h/\lambda_{LT} > 0.66$, then the energy of this mode propagates within more than a half wavelength in the layer close to the surface; the displacement becomes that of a Rayleigh wave in the $Si_3N_4$ material. Hence, the value deduced from the saturated region corresponds to that of $Si_3N_4$ thick layer: $(V_R)_{Si_3N_4} = 5694$ m/s.

Therefore, it is safe to consider that the transition normalized thickness, $(h/\lambda_{LT})_{tr}$, separating both regions, corresponds to the first layer thickness at which the velocity becomes constant, i.e. at the threshold of the saturation of region II, evaluated in this case to be $(h/\lambda_{LT})_{tr} = 0.66$.

## 3. Results and discussion

### *3.1. Different layers on the same SiC-substrate*

Let us first consider the effects of different loading layers ($Al_2O_3$, $SiO_2$, $Si_3N_4$, AlN, TiN, Al, W, Fe, Ti, Mg, Cu, V, Monel, Inconel, Heavy-flint) deposited on the same substrate (SiC). Typical results of Rayleigh velocity, $V_R$, values for some of the investigated layers ($Al_2O_3$, $SiO_2$, Ti and W) are displayed in Fig. 2 as a function of normalized film thickness, $h/\lambda_{LT}$. It is clear that the curves of all layer/substrate combinations show similar behavior: an initial decrease followed by a saturation region. The highest velocity value is obtained at the onset of the decreasing region

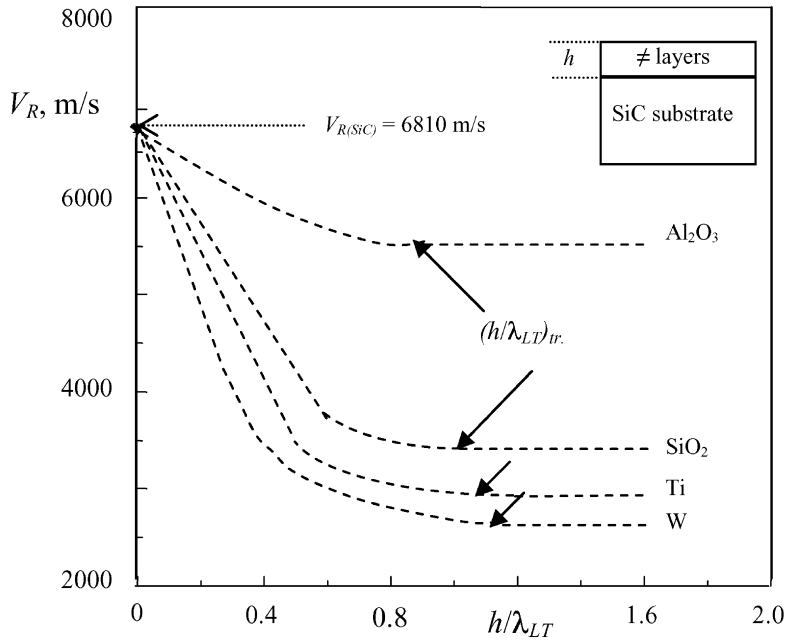


Fig. 2. Velocity dispersion curves for $Al_2O_3$/SiC, $SiO_2$/SiC, Ti/SiC and W/SiC; the arrows indicate the normalized thickness transition, $(h/\lambda_{LT})_{tr}$, beyond which the SAW propagates completely in layers.

corresponding to a negligible layer thickness. Thus, most of the energy is carried in the substrate [15,18] and the displacement is characteristic of a Rayleigh wave on an SiC free surface, i.e. $V_{R(SiC)} = 6810$ m/s in agreement with literature [10]. As the values of $h/\lambda_{LT}$ begin to increase, the velocity decreases sharply; this velocity represents that of the whole thin film/substrate structure. The detailed variation in velocity depends on a number of physical and elastic parameters. These may be related to bulk properties of the materials involved, to the fabrication conditions e.g. differential interface stress and/or to subsequent adhesion-related phenomena that affect bound strength, etc. [15,19].

For large $h/\lambda_{LT}$, the velocity values of each curve tend asymptotically towards a constant value. The saturation corresponds to Rayleigh wave on each layer which becomes thick enough to behave as bulk material. Hence, one can easily deduce from the saturated curves that: $V_{R(Al_2O_3)} = 5680$ m/s, $V_{R(SiO_2)} = 3410$ m/s, $V_{R(Ti)} = 2960$ m/s and $V_{R(W)} = 2670$ m/s, in good agreement with literature [10] with differences of less than 1%.

However, the transition from decreasing region to saturated region (indicated by arrows in Fig. 2) occurs at different normalized thickness, $(h/\lambda_{LT})_{tr}$; thus, characterizing each layer/SiC combinations. Therefore, in the present case of a single substrate, the variations in the values of transition thickness are due to differences in the acoustic properties of such layers.

### *3.2. Same Ti-layer on different substrates*

To enrich this investigation and to put, even more, into evidence this effect, we considered other types of substrates (Be, $Al_2O_3$, AlN, Si, $SiO_2$, Mg, TiN, WC, and Pyrex) onto which a great number of layers were deposited. Fig. 3 illustrates typical dispersion curves obtained with Ti layers deposited on Be, SiC, Si, or WC. It can be seen that the dispersion trend (an initial decrease followed by a saturation region) is obtained for all combinations. All the curves saturate at the same Rayleigh velocity that corresponds to that of Ti layer, $V_{R(Ti)} = 2950$ m/s; this behavior happens when Ti becomes thicker than the wavelength of the propagating mode. Whereas, their initial decrease start at different Rayleigh velocities that correspond to that of the corresponding substrate, i.e., $V_{R(Be)} = 7840$ m/s, $V_{R(SiC)} = 6810$ m/s, $V_{R(Si)} = 4710$ m/s and $V_{R(WC)} = 3640$ m/s. The main difference, in such curves lies in the position of the normalized thickness at which the saturation sets in. Hence, as in Fig. 2, the transition to saturated regions (indicated by arrows) occurs at different normalized thickness, $(h/\lambda_{LT})_{tr}$; thus, characterizing the structures Ti layer on different substrates.

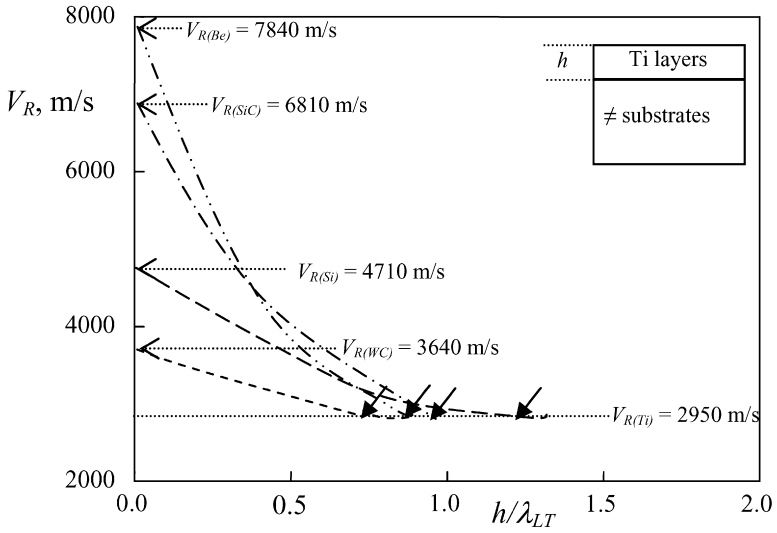


Fig. 3. Velocity dispersion curves for Ti/Be, Ti/SiC, Ti/Si and Ti/WC; the arrows indicate the normalized thickness transition, $(h/\lambda_{LT})_{tr}$, beyond which the SAW propagates completely in the layer.

It is worth noting that these observations were also obtained with several other layers deposited on many different substrates. Hence, it is safe to say that densities and SAW velocities of both layers and substrates are responsible for the discrepancies in the values of critical thickness at which transitions occur. It should be noted that similar dispersive behaviors were experimentally observed for several layers/substrate combinations [8–10,15,17].

## 4. Determination of the critical thickness

### *4.1. Quantification of the onset of layer characteristics*

To quantify the effects of elastic parameters (velocities and densities, $\rho$) on the onset of thickness transition and in order to make valuable comparison between various structures and combinations, we introduce a parameter, $\chi$, defined as: $\chi = (V_{RL}/V_{RS})/(\rho_L/\rho_S)$; subscripts S and L are used to designate the quantities concerned with the substrate and the layer, respectively. Thus, $\chi$ is a combined parameter that characterizes each layer/substrate structure. To compare the results obtained with different fast substrates (Be, $Al_2O_3$, AlN, SiC, TiN) and various loading layers, in Fig. 4 we plot the critical transition thickness $(h/\lambda_{LT})_{tr}$ as a function of $\chi$ for a great number of loading layers deposited on Be, SiC or TiN substrates. A linear decrease is clearly obtained in all cases; the line of best fit gives a linear analytical formula, for different fast substrates, as follows:

– Be substrates:

$$(h/\lambda_{LT})_{tr} = -1.25(\chi)_{Be} + 1.2 \tag{1}$$

– SiC substrates:

$$(h/\lambda_{LT})_{tr} = -0.49(\chi)_{SiC} + 1.14 \tag{2}$$

– TiN substrates:

$$(h/\lambda_{LT})_{tr} = -0.12(\chi)_{TiN} + 1.15 \tag{3}$$

However, for slow substrates, the curves of $(h/\lambda_{LT})_{tr}$ versus $\chi$, displayed in Fig. 5, showed the inverse behavior i.e., $(h/\lambda_{LT})_{tr}$ increases with increasing $\chi$ for loading layers deposited on typical slow substrates: WC, $SiO_2$ and Pyrex, giving the following variations:

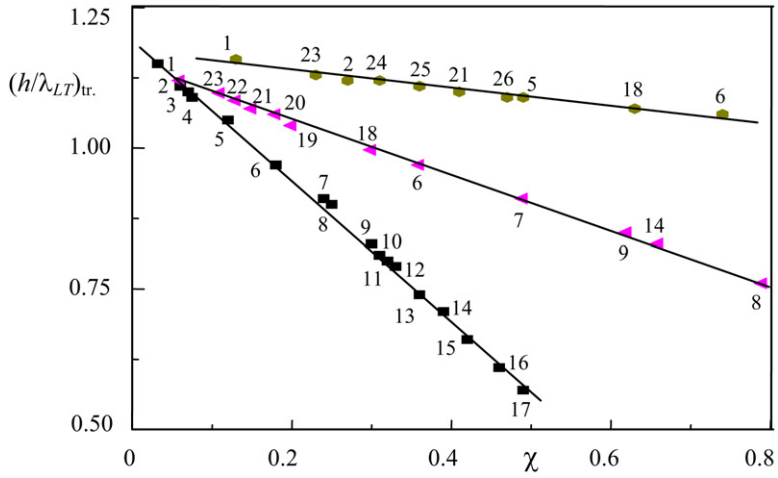


Fig. 4. Critical transition thickness, $(h/\lambda_{LT})_{tr}$, as a function of the parameter $\chi = (V_{RL}/V_{RS})/(\rho_L/\rho_S)$. Line of best fit (– – –). Numbers (1–26) represent the deduced values of the following loading layers deposited on Be (■), SiC (◄) or TiN (●) substrates: (1) W; (2) Constantan; (3) Zn; (4) Mo; (5) Cr; (6) Heavy flint; (7) TiN; (8) Al; (9) $SiO_2$; (10) Pyrex; (11) $Al_2O_3$; (12) MgO; (13) Quartz; (14) Mg; (15) $Si_3N_4$; (16) AlN; (17) SiC; (18) Ti; (19) Fe; (20) V; (21) Monel; (22) Inconel; (23) Cu; (24) Zr; (25) Stainless steel; (26) ZnO.

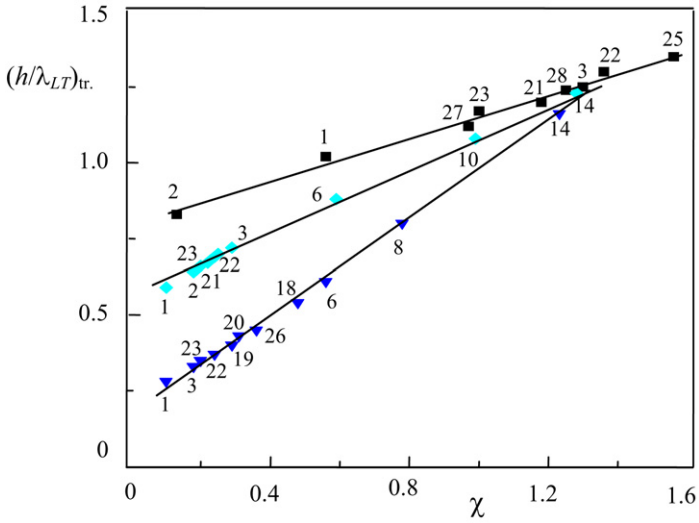


Fig. 5. Critical transition thickness, $(h/\lambda_{LT})_{tr}$, as a function of the parameter $\chi = (V_{RL}/V_{RS})/(\rho_L/\rho_S)$. Line of best fit (– – –). Numbers (1, etc.) represent the deduced values of the following loading layers deposited on WC (■), $SiO_2$ (▼) or Pyrex (♦) substrates: (1) W; (2) Constantan; (3) Zn; (6) Heavy flint; (8) Al; (10) Pyrex; (14) Mg; SiC; (18) Ti; (19) Fe; (20) V; (21) Monel; (22) Inconel; (23) Cu; (25) Stainless steel; (26) ZnO; (27) Zircolay; (28) Ni.

– WC substrates:

$$(h/\lambda_{LT})_{tr} = 0.35(\chi)_{WC} + 0.78 \tag{4}$$

– $SiO_2$ substrates:

$$(h/\lambda_{LT})_{tr} = 0.52(\chi)_{SiO_2} + 0.56 \tag{5}$$

– Pyrex substrates:

$$(h/\lambda_{LT})_{tr} = 0.81(\chi)_{Pyrex} + 0.17 \tag{6}$$

Table 1
Characteristic constant values in the relationship: $(h/\lambda_{LT})_{tr} = \alpha\chi + \beta$ for different loading layers deposited on slow and fast substrates; Mx is a fictitious substrate material

| | Slow substrates | | | | | | Fast substrates | | | | |
|---|---|---|---|---|---|---|---|---|---|---|---|
| | Pyrex | Mg | $SiO_2$ | WC | Si | Mx | TiN | AlN | $Al_2O_3$ | SiC | Be |
| $\alpha$ | +0.81 | +0.65 | +0.52 | +0.35 | +0.16 | 0.0 | −0.12 | −0.23 | −0.38 | −0.49 | −1.25 |
| $\beta$ | 0.17 | 0.37 | 0.56 | 0.78 | 1.16 | 1.15 | 1.15 | 1.16 | 1.15 | 1.14 | 1.20 |
| $V_{RS}$ | 3013 | 2930 | 3410 | 3643 | 4712 | 5046 | 5367 | 6418 | 5680 | 6810 | 7844 |

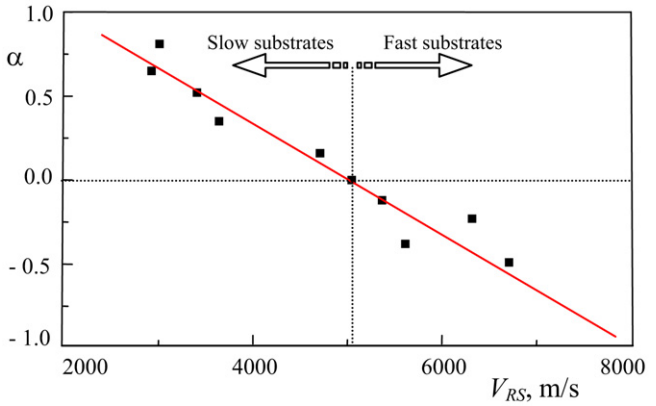


Fig. 6. Characteristic slope, $\alpha$, as a function of $V_{RS}$ for several investigated layer/substrate combinations.

### 4.2. Analytical formula generalization

It is very important to stress that all variations obtained with loading layers deposited on both slow and fast substrates (relations (1)–(6)) can be expressed by a linear dependence of the form:

$$\left[\frac{h}{\lambda_{LT}}\right]_{tr} = \alpha\chi + \beta = \alpha\frac{V_{RL}/V_{RS}}{\rho_L/\rho_S} + \beta \tag{7}$$

where $\alpha$ and $\beta$ are characteristic constants for a given substrate over which different layers are deposited; such constants are summarized in Table 1 for all investigated substrates; included in the table are the values of $V_{RS}$ for discussion. Close analysis of the values of $\alpha$ shows that for fast substrates the slope is not only negative but gets stronger as the substrate becomes faster, whereas, for slow substrates the slope is positive and becomes stronger as the substrates become slower.

This behavior is better illustrated in Fig. 6, in terms of the characteristic slope, $\alpha$, as a function of $V_{RS}$ for the investigated layer/substrate combinations. It can be seen that as $V_{RS}$ decreases the parameter $\alpha$ increases for both slow and fast substrates. It should be noted that, it is possible to predict from Fig. 6 the material whose critical elastic values (velocities and density) correspond to the change from negative to positive behavior by considering a null slope, $\alpha = 0$. Thus, it was found that such a fictitious material, Mx, would be characterized by: $\rho = 3750$ kg/m$^3$, longitudinal velocity, $V_L = 9370$ m/s, transverse velocity, $V_T = 5490$ m/s and $V_R = 5046$ m/s; the values of these propagating wave velocities can be considered as the limiting case for not only differentiating between slow and fast substrates but also for the change from negative to positive behavior of $\alpha$ and vice versa.

The importance of relation (7) lies in its simplicity and its applicability to all types of loading-layer/substrate combinations. Moreover, it is expressed in terms of known and/or measurable physical parameters (only densities and velocities). Therefore, it could be used to predict the critical transition thickness at which the elastic parameters of layers dominate. This thickness is of great importance in choosing operating conditions in acoustic microscopy. The physical phenomena governing such a relation remain those responsible for velocity dispersion in any layer/substrate combination (Section 2.2) whose combining effect was regrouped in a single acoustic parameter, $\chi$. Moreover, this proposed formula can be considered as an alternative procedure to predict and deduce critical thickness values, without

any prior calculation of velocity dispersion curves. Thus, by just knowing elastic parameters of the substrate and the layer, one can easily determine the thickness beyond which surface acoustic waves propagate completely in the loading layer.

## 5. Conclusions

It is shown that densities and velocities of both layers and substrates play an important role in the determination of the critical thickness at which the characteristics of loading layers become dominant. Such a role is quantified by an interesting linear expression (7) which can be applied to all types of loading layers/substrates combinations. The proposed formula can be considered as an alternative straightforward method to predict and deduce critical thickness values, without any prior calculation of velocity dispersion curves. Thus, by just knowing elastic parameters of the substrate and the layer, one can easily determine the thickness beyond which surface acoustic waves propagate completely in the loading layer.

## References

[1] G.W. Farnell, E.L. Adler, in: R.N. Thurson, P.W. Mason (Eds.), Physical Acoustics, vol. X, Academic Press, New York, 1972, pp. 35–127.
[2] J.L. Rose, Ultrasonic Waves in Solid Media, Cambridge Univ. Press, Cambridge, 1999.
[3] Z. Yu, S. Boseck, Rev. Mod. Phys. 67 (1995) 863.
[4] I. Touati, Z. Hadjoub, A. Doghmane, Phys. Chem. News 27 (2006) 26.
[5] A.G. Every, Meas. Sci. Technol. 13 (2002) R21.
[6] W.-S. Ohm, M.F. Hamilton, J. Acoust. Soc. Am. 115 (2004) 2798.
[7] Z. Hadjoub, I. Beldi, M. Bouloudenine, A. Gacem, A. Doghmane, Electron. Lett. 34 (1998) 313.
[8] J.D. Achenbach, J.O. Kim, Y.-C. Lee, in: A. Briggs (Ed.), Advances in Acoustic Microscopy, vol. 1, Plenum Press, New York, 1995, pp. 153–208.
[9] J.O. Kim, J.D. Achenbach, P.B. Mirkarimi, S.A. Barnett, J. Appl. Phys. 72 (1992) 1805.
[10] A. Briggs, Acoustic Microscopy, Clarendon Press, Oxford, 1992.
[11] Z. Hadjoub, I. Beldi, A. Doghmane, C. R. Physique 8 (2007) 948.
[12] J. Kushibiki, N. Chubachi, IEEE Sonics Ultrason. SU-32 (1985) 189.
[13] C.J.R. Sheppard, T. Wilson, Appl. Phys. Lett. 38 (1981) 858.
[14] P.V. Zinin, in: M. Levy, H. Bass, R. Stern (Eds.), Handbook of Elastic Properties of Solids, Liquids and Gases, vol. 1, Academic Press, New York, 2001, pp. 187–226.
[15] A. Doghmane, Z. Hadjoub, F. Hadjoub, Thin Solid Films 310 (1997) 203.
[16] L. Adler, in: J.D. Achenbach (Ed.), Evaluation of Materials and Structures by Quantitative Ultrasonics, Springer-Verlag, Wien, 1993, pp. 133–147.
[17] J.D. Achenbach (Ed.), Evaluation of Materials and Structures by Quantitative Ultrasonics, Springer-Verlag, Wien, 1993.
[18] G.W. Farnell, in: A.A. Oliner (Ed.), Acoustic Surface Waves, Springer-Verlag, Berlin, 1978, pp. 13–60.
[19] B.W. Maxfield, R.D. Weiglein, Ultrasonic Symposium, IEEE, New York, 1981, p. 561.